Personalised Medicine in Cervical Cancer: Evaluating Therapy Resistance Through Multi-Model Approaches

Meyer M, Eksteen C, de Sousa C, et al. | Cancer Medicine, 2025 | DOI: 10.1002/cam4.70995

CancerMedicine

Personalised Medicine in Cervical Cancer: Evaluating Therapy Resistance Through Multi-Model Approaches

Madré Meyerl D | Carla Eksteen1 | Cayleigh de Sousa1 @ ｜ Nireshni Chellan2 @ | Ruzayda Van Aarde2 | Meenal Bhaga1 ↓ Johann Riedemann3 I Matthys H. Botha3 | Frederick H. van der Merwe4 I Anna-Mart Engelbrecht1 @

Department of Physiological Sciences, Stellenbosch University, Cape Town, South Africa I 2South African Medical Research Council (SAMRC), Cape Town, South Africa I 3CancerCare, Cape Gate Oncology Centre, Cape Town, South Africa I +Department of Obstetrics and Gynecology, Stellenbosch University, Stellenbosch, South Africa

Correspondence: Anna-Mart Engelbrecht (ame@sun.ac.za)

Received: 4 March 2025 I Revised: 8 May 2025 I Accepted: 26 May 2025

Funding: This work was financially supported by the South African Medical Research Council (SAMRC) (A.M.-E.), the Cancer Association of South Africa (CANSA) (A.M.-E.), the Technology Innovation Agency (TIA) and the National Research Foundation (NRF) of South Africa grant 138118 (A.M.-E.).

Keywords: cervical cancer I personalised medicine I senescence | treatment resistance

ABSTRACT

Introduction: Cervical cancer remains a leading cause of malignancy among women globally, disproportionately affecting women from low-to-middle-income countries, including South Africa. The high prevalence in impoverished communities places significant pressure on the public healthcare system. In these regions, human papillomavirus (HPV); the primary risk factor for cervical cancer—along with co-occurring immunosuppressive conditions such as HIV, is common. Compounding this burden is the widespread development of treatment resistance to conventional therapies like cisplatin and carboplatin. Resistance is fre- quently associated with therapy-induced cellular senescence, underscoring the need for more personalised treatment strategies tailored to individual patient profiles.

Methods and Materials: This study aimed to assess ex vivo methods' utility in predicting patient-specific therapy responses. Biopsy samples from cervical cancer patients were cultured and subjected to various chemotherapies. Cell viability, senescence markers and treatment resistance pathways were analysed to determine optimal treatment outcomes.

Results: The findings revealed significant variability in optimal treatment responses, with ex vivo methods demonstrating limitations in fully capturing the complexity of patient-specific reactions to therapy. No single experimental model provided comprehensive predictive insights into treatment outcomes.

---CHUNK_BREAK---

Conclusion: This study underscores the need for integrative and multidisciplinary approaches when evaluating treatment strat- egies for cervical cancer. While ex vivo models offer valuable insights, combining multiple experimental methods is crucial for a more reliable and comprehensive understanding of treatment response and resistance mechanisms. Standardiszing approaches or employing method combinations may enhance personalised medicine efforts, particularly in resource-limited settings.

in Sub-Saharan Africa, primarily due to the high prevalence of

1| Introduction

Human Papillomavirus (HPV) infection, particularly oncogenic

Cervical cancer ranks as the fourth most prevalent malignancy

subtypes HPV-16 and HPV-18 [3]. Despite advancements in

among women worldwide [1], with a disproportionate impact

screening and HPV vaccination, cervical cancer remains a major health threat. A key factor contributing to treatment resistance

on low-to-middle-income countries (LMICs) like South Africa [2]. It is the leading cause of cancer-related death among women

is oncogene-induced senescence, a hallmark of cancer, defined

as a state of irreversible growth arrest triggered by endogenous

Primary cell cultures offer a more accurate representation of

and exogenous stressors. Senescent cells can accumulate in cer-

the tumour microenvironment but pose challenges such as slow

vical tissues, creating a tumour-promoting microenvironment proliferation, poor adherence, fibroblast overgrowth, contamination risks and limited passage numbers [7]. Despite optimisation attempts, only 50%-60% of patient samples reached a viable stage for experimentation, complicating efforts to determine optimal treatment responses. These challenges are further discussed in subsequent sections.

via the activation of pathways such as pl6/Rb and secretion of senescence-associated secretory phenotype (SASP) proteins [4, 5]. This senescent phenotype is linked to chemotherapy resistance and cancer recurrence via multidrug resistance muta- tion 1 (MDR1) and ATP binding cassette subfamily G member 2 (ABCG2) [6]. However, the role of senescence-induced treat- ment resistance in cervical cancer remains poorly understood, underscoring the need for innovative approaches, such as personalised medicine, to enhance our understanding thereof. We hypothesised that patient-derived biopsies could facilitate personalised treatment predictions. This study aimed to investigate this association using an ex vivo approach to assess individual cervical cancer patients' chemotherapy responses, emphasising the importance of multidisciplinary methodologies in personalised medicine.

2 | Methods and Materials

2.1 I Patient Recruitment

Ethical approval was granted by Stellenbosch University (HREC—N22/04/037). Participants were recruited from Tygerberg Hospital's Obstetrics and Gynaecology outpatient clinic, where they provided informed consent. Inclusion criteria were: (1) advanced cervical cancer diagnosis, (2) female at birth, (3) fluent in English, Afrikaans or isiXhosa, (4) 18years or older, (5) no history of other cancers and (6) treatment-naive status. Patients were not excluded based on socioeconomic background, education level or race. Identities were anonymised using unique identifiers.

2.2 I Collection of Specimens

During routine staging (based on the International Federation

2.4 | Treatment Protocol

Six treatment groups were used, along with the patient controls: (1) 0.005 µM Paclitaxel (Pxt), (2) 1µM Doxorubicin (Dxr), (3) 3.3 µM Gemcitabine (Gem), (4)12 µM Carboplatin (Carbo),(5)12µM Carbo +0.005 µM Pxt and (6) 12 µM Carbo +3.3 µM Gem. Low-dose chemotherapy levels were selected based on the literature [8-10].

2.5 | WST-1 Cell Viability Assay

Cell metabolic activity was assessed using the WST-1 assay (Merck, Sigma-Aldrich). The reagent was added (1:10 ratio) and incubated for 4h, after which absorbance was measured at 450 nm using an EL 800 Universal Microplate Reader.

2.6 I Western Blots

Protein extraction was performed 72h post-treatment. Cells were washed with PBS, lysed in modified RIPA buffer and centrifuged at 4°C. Protein quantification was done using the Bradford Assay. Samples were prepared in Laemmli buffer and run on 12% resolving and 4% stacking gels (Bio-Rad TGX Stain- Free FastCast Kit). Membranes were blocked in 5% Bio-Rad Blocking Buffer, incubated with primary antibodies (MCM2, p16, ABCG2, MDR1, p38, Rb, p-Rb; Cell Signalling Technology), and treated with secondary antibodies (1:10,00o dilution).

Chemiluminescent signals were detected using Image Lab soft-
of Gynaecology and Obstetrics [FIGO] system) small cervical
ware and normalised to GAPDH.
tumour biopsies (±1 to 2g) were collected, placed in Dulbecco's Modified Eagle Medium (DMEM), and kept on ice. Samples were processed at Stelenbosch University's Department of
2.7 I Senescent Phenotype Determination via Senescence-Associated Beta-Galactosidase (SA-B-
Physiological Sciences, mechanically dissociated, and cultured
Gal) Staining Kit
until confluency before being seeded into culture flasks and treated with low-dose chemotherapy. A retrospective analysis of patient data was performed to explore correlations between
SA-β-gal staining (Cell Signalling Technology) was performed
senescence markers and treatment responses.
72h post-treatment to assess senescence. This histochemical assay detects β-galactosidase, a lysosomal enzyme expressed in senescent cells at pH6 [11]. Cervical cells (10,000 per well) were
2.3 | Primary Cell Culture
seeded in 12-well plates, treated, fixed and stained per the man- ufacturer's protocol, and then incubated overnight without CO2.
As seen in Figure 1, tumour biopsies were mechanically disso-
Staining was visualised using a Zeiss phase-contrast microscope
ciated, incubated with 0.25% Trypsin-EDTA, centrifuged at
and analysed with ImageJ (FIJI).
1500rpm for 3min, and seeded into 6-well plates containing DMEM/F12 (50:50) supplemented with 10% fetal bovine serum,
2.8 ↑ Blood Plasma Inflammatory Profiling
1% Penicillin-Streptomycin and 1% Amphotericin (Gibco, ThermoFisher Scientific). Cells were cultured at 37°C with 5% CO2 and monitored for contamination and successful attach-

---CHUNK_BREAK---

Visual Type: Flowchart

Title: Instructions for using the machine

Data Points: 7 steps as indicated by numbered blocks on the flowchart.

Captions / Annotations:
1. "Chemical" with a picture of a test tube.
2. "Adding media to centrifuge" with an image of a centrifuge and media.
3. "Adding cells into a well plate" showing a well plate with cells.
4. "Incubating at 37 degrees Celsius" with a temperature display reading 37 degrees.
5. "Washing the cells to remove debris."
6. "Disaggregation of cancer cells and addition of media."
7. "Adding cells into well plates for subtraction into a plate."solution.

FIGURE 1 I Protocol for the dissociation and processing of primary cervical tumour biopsies (made with BioRender). HBSS, Hank's buffer saline
①Harvest cervical
2Cutbiopsiesinto
③Rinsecutbiopsieswith
biopsies
smallerpieces
HBSS
Add media to
Centrifugetube
④ Incubate in trypsin for
toform
neutralisetrypsin

20-30 mins @ 37°°C
supernatant
withagitationfor
disaggregation of
fibroblasts
Incubatetoallow
Seed cell
suspension into a
appropriate
8
attachmentand
6-wellplate
proliferation of cancer
once cells grow
cells(5-7 days)
confluntnlate,lit
intoaT25,andfrom
thereintoaT75

---CHUNK_BREAK---

Inflammatory cytokines (IL-1β, IL-6, TNF-α, VEGF-α, IFN)
ment. Once 75% confluency was reached, cells were trypsinised
were quantified using the Milliplex MAP Human Cytokine/ Chemokine Magnetic Bead Panel (Merck). Plasma samples were
and reseeded.
cultures, while also highlighting the importance of employing
thawed from -80°C to -20°C.Beads bound to analytes were in- cubated with biotinylated antibodies and Streptavidin-PE, then
integrative and more advanced methods.
analysed via Luminex flow cytometry.
A 32-year-old woman, referred to as ‘the patient', was diagnosed with stage 3B cervical squamous cell carcinoma (SCC) during a
2.9|Statistical Analysis
staging appointment at Tygerberg Hospital (Cape Town, South Africa). This is unusually young for such an advanced diagnosis [12].
More than 95% of cervical SCC cases are HPV-positive, a
Visual representation and statistical analysis of the data were generated using GraphPad Prism version 9 for Mac OS X
figure even higher in sub-Saharan Africa. The patient was also HIV-positive, a co-infection that increases the likelihood of cer-
(GraphPad Software, San Diego, CA). All the values represented were expressed as a percentage of the control ± standard error
vical cancer by up to six times [13]. Following staging and ob-
of the means (SEM). Significant differences were assessed by
taining informed consent, a cervical tumour biopsy was taken
one-way analysis ofvariance (ANOVA) using the Tukey post hoc
and processed for further analysis as described in Section 2.1.
test. A p-value < O,05 was considered statistically significant.
3.1|Cell Viability Assay
3 | Case Report for the Patient
Absorbance results of the cellular viability assay are presented
This case provides valuable insights into the potential of our
in Figure 2 and are expressed as a percentage of the patient con-
approach, even within the limitations faced with primary cell
trol. There was a significant reduction in cellular viability in all
2045 7634, ,13,
the chemotherapy groups, except for the Pxt treatment group.
Additionally, the greatest reduction in cell viability was seen in the Dxr group (p<0,0001) and the Carbo + Gem combination

---CHUNK_BREAK---

GENERAL FIGURE CONTENT:

The figure consists of two separate images presented side by side. On the left, there is a bar chart with horizontal bars, each representing a different data point. The bars are color-coded and appear to be related to some form of health or medical data, as suggested by terms like "Patient," "WST2," "Senescence," and "Apoptosis."

Below the bar chart, there is text that reads "The Patient WST2 Metabolic Stress Screen: Senescence." This suggests a connection between the metabolic stress screen (WST2) and senescence in the context of patient health.

On the right side of the image, there is a series of icons or markers connected by lines, forming a network or pathway. The exact meaning or function of these connections is not clear from the image alone.

The figures are presented against a white background with black text and graphics, which is standard for printed or digital documents. There appears to be a watermark or logo in the lower right corner of both images, but it is too small to discern any specific details about it.Pxt, paclitaxel.
p<0.0001. Carbo, carboplatin; Dxr, doxorubicin; Gem, Gemcitabine;
The asterisk (*) denotes p<0.05, (**) denotes p<0.01 and (****) denotes
senescence induction. Results are presented as means ± SEM (n=3).
sity of 5000 cells per well and treated for 72h to allow for appropriate
determined via WST-1 assay. The patient's cells were seeded at a den-
FIGURE 2 I Percentage viability of the patient cells after treatment
The Patient: WST-1
****
*
**
**
150
control)
****
6
100-
Il viability
50-
Cell
MT
M
M
M
12
00
G
Q
UIMI
UMI
12
? °
C
Chemotherapy concentrations

---CHUNK_BREAK---

Visual Type: Bar Chart

Title: Cognitive Impacts of COVID-19 Intervention Strategies
Axes / Legends / Labels:
- X Axis: Strategy
- Y Axis: Impact Score (%)
Data Points:
- Control
- Strategy 1
- Strategy 2
- Strategy 3
Captions / Annotations:
- Each bar represents a different cognitive impact of the intervention strategy.
- The heights of the bars indicate the percentage improvement or decline in each area compared to the control strategy.
- There are three strategies represented on the x axis, each with a corresponding set of bars indicating its cognitive impacts. Pxt, paclitaxel.
p<0.0001. Carbo, carboplatin; Dxr, doxorubicin; Gem, Gemcitabine;
are presented as means ± SEM (n=3). The asterisk (****) denotes
was no significant senescence induction in the control group. Results
induction of senescence in all the chemotherapy-treated groups. There
72h to allow for appropriate senescence induction. There is a significant
Cells were seeded at a density of 10,000 cells per well and treated for
tion in the patient cells, determined via beta-galactosidase staining.
FIGURE 3 | Percentage chemotherapy-induced senescence induc-
The Patient Beta-galactosidase stain: Senescence induction
****
****
****
****
100)
****
80
****
out
60
induction
40
5
Chemotherapy concentrations

---CHUNK_BREAK---

these promising results, Gem and Carbo's combinations remain
treatment group (p<0,0001).
outside South Africa's standard treatment protocols [14].
Dxr treatment exhibited the most significant decrease in cell vi- ability (p<0.00o1). Carbo, Pxt, Gem and/or combinations are
3.2 I SA-B-Gal Staining for Confirmation
typically administered for cervical cancer patients. Tygerberg
of Senescence Induction
Hospital, where the patient's samples were obtained, exclusively administers platinum-based chemotherapy, cisplatin, with adju- vant radiation therapy [14]. Nevertheless, there is evidence of stud-
Senescent cells show increased lysosomal activity, including higher SA-B-gal levels, which thrive at a pH of 6 [11], making
ies that investigated the use of Dxr on cervical cancer cell lines; for
SA-B-gal a key marker for senescence. To confirm senescence
example, a study by Bano et al. [15] demonstrates that Dxr, com- bined with Chloroquine, reduces cell viability and increases apop-
induction in the treatment groups, SA-B-gal staining was per-

tosis in HeLa cells. However, challenges with Dxr, including poor formed (Figure 3). Results are expressed as a percentage out of solubility and severe side effects like myocardial infarctions, often 100, showing significant senescence induction in all chemother- apy groups compared to the control. Representative images are limit its clinical use [16]. In this study, Carbo reduced cell viability shown in Figure 4.
by approximately 40% compared to the control ($p<0.01$), whereas Dxr reduced viability by about 75%. Combination therapies further SA-B-gal forms when substrates like lactose and sphingolip-
showed promise. The Carbo + Gem group achieved a greater re- duction in viability (~70%, $p<0.0001$) than Carbo alone, consistent ids are cleaved by the B-gal enzyme. This lysosomal hydrolase is visualised by staining with an SA-B-gal kit (Cell Signalling with studies on SiHa and CaSki lines that highlight synergistic
Technology), producing a blue dye. The observed senescence interactions between Gem and Carbo [17]. Similar findings have

---CHUNK_BREAK---

MODE 1: STRUCTURED VISUAL DATA OUTPUT

Visual Type: Bar chart
Title: Unknown
Axes / Legends / Labels: Axes not visible, labels likely to indicate data types or categories, but are not legible in the image.
Data Points: Numerical values represent a quantity of cells with different shapes and sizes for each condition (a - h).
Captions / Annotations: The chart displays the number of each cell type at 20 hours of incubation under various growth conditions (a - h).

MODE 2: GENERAL FIGURE CONTENT

- This image is a composite of multiple photographs or data representations, possibly taken from different parts of a report or presentation.
- The central figure shows a bar chart with numerical values indicating the number of cells for each growth condition (a - h).
- To the left and right of the central chart are images showing microscopic cells under the various conditions. These images feature cells with different shapes, sizes, and densities, consistent with the data in the chart.
- The images showcase a variety of cell morphologies that may be indicative of differentiation states or responses to growth factors.
- There is no visible text or labels within the images providing additional context or analysis.on a Zeiss phase contrast microscope.
Carbo, carbo-platin; Dxr, oxorubicin; Gem, emcitabine; Pxt, aclitaxel.
FIGURE 4 I Images of senescence induction via beta-galactosidase staining. Images were acquired at a 10xX magnification (scale bar of 100 μm)
A:Control
B: Pxt
100 μm
100 μm
D: Gem
C: Dxr
100 μm
100μm
F: Carbo
E:Carbo
+Gem
100 μm
100 μm
G: Carbo
+ Pxt

100 µm

---CHUNK_BREAK---

induction across all treatment groups aligns with the WST-1
been reported for cisplatin and Gem combinations [18]. Despite
results, which showed reduced cell viability. Notably, Pxt
The Carbo + Pxt group showed increased MCM2 expression,
had the lowest senescence induction and reduction in
indicating activation of proliferation pathways. In contrast,
cell viability. However, similar senescence levels across
reduced MCM2 levels were observed in the other treatment groups, aligning with the WST-1 results (Figure 2) and suggest-
treatments highlight the need to analyse specific markers to better understand the underlying mechanisms and pathway
ing decreased proliferation. The Dxr group showed the lowest MCM2 expression, followed by Carbo. Although Carbo is widely
activation.
preferred for cervical cancer treatment, its cell viability results did not reflect this advantage. Nonetheless, the low MCM2 ex-
3.3 | The Effects of Senescence Induction on
pression may point to reduced proliferation in the Carbo group.
Cellular Proliferation
Western blot analysis of the proliferation marker MCM2,
Confirmation of Senescence Induction3.4
which regulates DNA replication and cell proliferation [19],
Markers
was conducted to investigate the observed changes in cell viability and senescence induction. A decrease in MCM2 ex-
To further validate senescence induction, western blot analysis examined key markers p16, Rb and p-Rb (Figure 6). The tumour
pression indicates reduced proliferation in the chemother- apy groups compared to the control. Figure 5 shows reduced
suppressor protein pl6, a regulator of the intrinsic senescence
MCM2 levels in the Pxt, Dxr, Gem, Carbo and Carbo + Gem
pathway, has strong associations with ageing and senescence [20]. Increased pl6 levels indicate heightened senescence
groups. An immortalised HPV-positive HeLa cell line served
through this pathway. Additionally, pl6 regulates the pl6-Rb
as a positive control.
pathway, with Rb playing a crucial role in cell cycle arrest by
particularly in the Dxr and Gem groups, may suggest a lower likelihood of treatment resistance. Similarly, decreased p-Rb:
associating with E2F and promoting hypo-phosphorylation.
The total Rb to p-Rb ratio serves as an indicator of hypo-

---CHUNK_BREAK---

MODE 2: GENERAL FIGURE CONTENT

The image shows a bar graph with numerical values representing counts of molecular groups. At the top of the bar graph, there is a title that reads "MCM2". The bars are labeled as follows: "400", "300", "200", "100", and "0" from left to right. Below the bars, there are labels indicating different molecular groups: "patient", "control", "cells", and "treatment". The graph is set against a white background with black text. There's also a watermark or logo in the lower-right corner of the image that seems to include a chemical structure, possibly related to the molecular groups mentioned.Pxt, paclitaxel.
protein, GAPDH. Carbo, carboplatin; Dxr, doxorubicin; GAPDH, glyceraldehyde-3-phosphate dehydrogenase; Gem, gemcitabine; kDa, kilodaltons;
flasks with the appropriate chemotherapy concentrations. Results are expressed relative to the patient control and normalised to a housekeeping
FIGURE 5 | Protein expression of proliferation marker MCM2 via western blot analysis. The patient cells were seeded and treated for 72h in T25
MCM2

400-
300
con
ent
200-
pat
the
100
to
Treatmentgroups
Protein
Patient
Carbo
Carbo
HeLa
Gem
Carbo
Pxt
Dxr
+Gem
standard
control
cells
+Pxt
MCM2
112kDa
3.11
1.00
0.25
0.75
0.35
1.03
0.78
0.67
GAPDH
36 kDa

---CHUNK_BREAK---

Rb expression in these groups further supports this possibility
phosphorylation, confirming senescence induction.
[22]. Interestingly, patients with lower senescence marker levels reportedly achieve better outcomes [23], suggesting the patient
All treatment groups showed decreased pl6 expression com-
in this study might benefit from treatment with Dxr, Gem or Carbo. Nonetheless, further evaluation of treatment resistance
pared to the control, with the greatest reduction in the Dxr group, followed by Gem and Carbo. This reduction suggests
markers is essential for drawing definitive conclusions.
decreased p16/Rb pathway activation. The p-Rb: total Rb ratio aligned with these findings, indicating increased Rb phosphor- ylation
and proliferative pathway activation rather than senes-
3.5|Determination of the Presence of Treatment
cence induction. These results contrast with SA-B-gal staining,
Resistance Markers
which confirmed senescence induction. However, it is possible
ABCG2 and MDR1 are key markers for assessing treatment
that an alternative senescence-induction pathway was activated during this experiment (such as the p21-p53 pathway and the

resistance, regulated in part by p38 signalling. ABCG2 acts
DNA damage pathway) or that these pathways were not actively
as a multidrug resistance transporter by expelling chemother-
engaged at the time of protein harvesting.
apeutics from cancer cells, while MDR1, an ATP-dependent transporter, plays a similar role in detoxification and re-
Research on chemotherapy and pl6 regulation in cervical can-
sistance [24]. An increase in these markers often indicates
cer is limited, though elevated pl6 levels have been linked to cis-
drug resistance. Figure 7 shows upregulated ABCG2 in both combination chemotherapy groups, with the Carbo + Pxt
platin resistance in SiHa cells [21]. The reduced pl6 expression,
MDR1 overexpression is a known prognostic marker for poor
group exhibiting the highest expression. MDR1 levels were highest in the Dxr group, followed by the combination groups.
outcomes in cervical cancer, with elevated levels linked to re-
Notably, p38 expression decreased across all treatment groups,
duced survival rates [27]. In this study, Dxr and the Carbo + Gem combination exhibited the highest MDR1 levels, suggest-
with the sharpest reductions in the Dxr, Pxt, Gem and Carbo

---CHUNK_BREAK---

MODE 1: STRUCTURED VISUAL DATA OUTPUT

Visual Type: Bar chart

Title: Total RB (total ribosomal binding)

Axes / Legends / Labels:

- X-axis: Protein groups
- Y-axis: Quantity of total RB

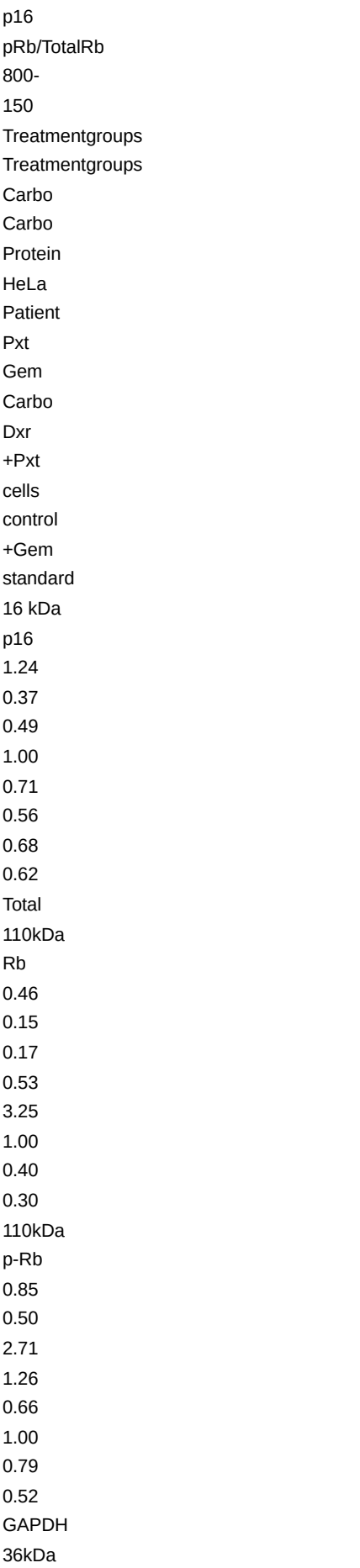
Data Points:

- Rb: 1675
- Hela: 408
- HeLa S3: 292
- Tet: 126
- C3: 101
- A270: 61
- A49T: 50
- A49: 29
- HCT11: 265
- DUO120: 248
- GAPDH: 384
- B2M: 227
- Actin: 305

Captions / Annotations:

- Protein groups are labeled along the x-axis.
- The y-axis indicates the quantity of total RB.
- Each bar represents a protein group and its corresponding value. GAPDH. Carbo, carboplatin; Dxr, doxorubicin; GAPDH,
glyceraldehyde-3-phosphate dehydrogenase; Gem, gemcitabine; kDa, kilodaltons; Pxt, paclitaxel.
in T25 flasks with the appropriate chemotherapy concentrations. Results are expressed relative to the control and normalised to a
housekeeping protein,

FIGURE 6|Protein expression of senescence markers pl6, Rb and p-Rb via western blot analysis.The patient cells were seeded and treated for 72h



---CHUNK_BREAK---

ing a potential association with poorer outcomes. Conversely,
groups.
Pxt and Carbo alone showed MDR1 levels closest to the con-
Chen reported basal ABCG2 expression in cervical cancer tis-
trol, indicating they may offer better treatment prospects. In a
sues, correlating higher levels with advanced disease stages
study by Ke et al. Nucleolin, a nucleocytoplasmic protein that is involved in the regulation of MDR1's efflux capabilities, mit-
[25]. Despite the patient being at stage 3B, no ABCG2 expres- sion was observed in the control sample. However, treatment
igated treatment resistance to cisplatin in HeLa cells in vitro
with Carbo, Carbo + Pxt and Carbo + Gem led to increased
[28]. However, the platinum-based chemotherapy from the cur-
ABCG2 expression, potentially linked to the cancer's advanced
rent study, Carbo, did not show the same effects. While cispla-
stage and a higher likelihood of developing treatment resis-
tin is associated with greater resistance and severe side effects, Carbo is better tolerated with comparable cytotoxic efficacy
tance. Notably, heightened ABCG2 expression did not align with the high MCM2 levels observed in combination groups,
[29]. Given the elevated ABCG2 expression with Carbo treat- ment, its efficacy in mitigating resistance remains uncertain.
which typically suggest proliferation. The unexpected ABCG2 increase in the Carbo group, despite low proliferation and se-
Therefore, the relationship between drug resistance and cyto-
nescence marker expression, could be explained by studies showing platinum-based chemotherapies' role in upregulating
toxicity remains complicated. In this patient, for instance, Dxr
ABCG2 in small-cell lung cancer [26]. Whether this effect ex-
treatment resulted in high MDR1 expression and correlating high cytotoxicity, as reflected in the cell viability assays. While this may
tends to cervical cancer remains unclear.
appear contradictory, since MDR1 is typically associated with drug
including cervical cancer [30]. Blood analysis (Figure 8) showed
efflux and reduced efficacy, it likely reflects Dxr's potent ability to
no significant differences from the control, except for a notable
induce rapid DNA damage and cell death, despite concurrently
reduction in VEGF-α ($p<0.001$).

---CHUNK_BREAK---

MODE 2: GENERAL FIGURE CONTENT

The image displays two different types of data representation: a bar chart and a line graph with error bars.

Bar Chart:
- The x-axis labels are "MND", "A963", and "A967".
- There are four distinct bars for each label, representing various groups or categories.
- The y-axis is labeled "Treatment groups", with values ranging from 0 to 1200.

Line Graph with Error Bars:
- The x-axis shows different treatments or groups.
- The y-axis is titled "Average value +/- SEM (standard error of the mean)".
- Data points are shown within the error bars, representing the statistical significance and variation in the data. Legend on next
page.FIGURE7 |
MDR1
ABCG2
1000

1500
800
1000
600
pati
400
500
Treatment groups
Treatment groups
p38
150-
100
C
Treatment groups
Carbo
Protein
Patient
Carbo
HeLa
Carbo
Pxt
Gem
Dxr
standard
control
cells
+Pxt
+Gem
72 kDa
ABCG2
3.46
1.63
8.57
1.00
0.35
0.77
0.65
1.68
MDR1
170 kDa
0.87
1.83
14.56
1.00
0.26
2.86
0.53
1.53
p38
38 kDa
0.83
1.00
0.80
0.55
0.55

0.57
0.62
0.45
GAPDH
36kDa

---CHUNK_BREAK---

MODE 2: GENERAL FIGURE CONTENT

The image displays various graphs with different data types. There are four distinct graphs within the frame.

1. The top left graph appears to be a scatter plot. It contains numerous data points, each represented by a small circle. These points are distributed across the graph, and there is a visible trend in their distribution.

2. Adjacent to it on the right, another graph seems to represent data in a bar chart format. The bars vary in height, with some being taller than others, suggesting a comparison or ranking of entities or categories.

3. Moving clockwise from the first graph, the third one is a line graph. It features a single line that curves upwards and then downwards, indicating fluctuations in values over time or across different data points.

4. Finally, the bottom left graph looks like a bar chart as well, but with a more pronounced horizontal distribution of bars. Each bar corresponds to a different category, and their lengths might indicate quantities or frequencies.

The image does not provide clear labels or titles for these graphs, so it's difficult to infer the specific context or data being represented.FIGURE 8 I Inflammatory profiling via Milliplex blood plasma analysis. (***p< 0,001).
kDa, kilodaltons; Pxt, paclitaxel.
to a housekeeping protein, GAPDH. Carbo, carboplatin; Dxr, doxorubicin; GAPDH, glyceraldehyde-3-phosphate dehydrogenase; Gem, gemcitabine;
sedrelativeto thecontrol andnormalised
and treated for 72h in T25 flasks with the appropriate chemothe
stern blot analysis.The patient cells were seeded
FIGURE 7 | Protein expression of treatment
IL-1β
TNF-α
VEGF-α
***
ns
ns
15
10
1500-
ml
10-
1000-
3
500
IL-6
IFN
20-
15-
ns
ns
15

(pg/ml)
ml
10
(pg/
10
IFN
6
5

---CHUNK_BREAK---

triggering cellular stress responses. This stress can upregulate MDR1 and promote cellular senescence. The elevated senescence
Advanced-stage cervical cancer patients often show elevated lev-
levels observed in the Dxr group reinforce the idea that while a
els ofIL-6, IL-1f and TNF-α [30, 31], though this was not observed
significant proportion of cells may undergo apoptosis, others may
for the patient. IFN levels also showed no significant reduction,
enter a dormant, therapy-resistant state. These findings highlight
aligning with findings from an Indian cervical cancer cohort
that short-term drug response does not always predict long-term
[32]. VEGF-α, typically elevated in solid tumours and linked to metastasis, angiogenesis and proliferation [33], was significantly
outcomes, highlighting the importance of evaluating multiple bio-
reduced ($p<0.001$). Zhang et al. associated high VEGF-α levels
logical endpoints when evaluating treatment outcomes.
with poor survival outcomes in cervical cancer [34]. Additionally, whole blood plasma analysis was performed (Table 1). While this alone
cannot provide definitive prognostic conclusions, it remains
3.6 ↑ Inflammatory Profiling via Blood Plasma Analysis
vital for guiding chemotherapy decisions and assessing overall health status.
Inflammatory markers IL-6, IL-1f, TNF-α, VEGF-α and IFN were assessed pre-treatment. These markers are linked to
The patient presented with a high white blood cell (WBC) count,
chronic inflammation, contributing to cancer progression,
while red blood cell (RBC) and platelet counts were normal. Choi
et al. identified baseline lymphocyte count as a key prognostic
5 |Organoid Culture
marker for cervical cancer, influencing response to concurrent chemotherapy and radiation [35]. Elevated WBC levels, often
As demonstrated by the results from the patient above and simi-
linked to inflammation, may impact coagulation and affect
lar findings observed in other patients from this study, definitive conclusions regarding optimal treatment strategies were chal-
chemotherapy outcomes. Although severe WBC elevation can lead to treatment-related toxicity in advanced cervical cancer
lenging to draw based solely on ex vivo experiments. To address
[36], this was not the case for the patient. The patient's elevated
this limitation, we advanced our approach by incorporating a
WBC count may also be attributed to their HIV-positive status,

---CHUNK_BREAK---

3D organoid cell culture model using patient biopsies. Three-
reflecting the immune response to ongoing infection [37]. These
dimensional cancer culturing models are gaining traction due
results should be interpreted alongside other findings for a com-
to their enhanced ability to mimic in vivo tumour conditions.
prehensive assessment.
Multiple studies have demonstrated that 3D models offer valu- able insights into cancer biology and facilitate the identification of cancer

cell biomarkers [38-40]. One significant advantage of

4 | The Patient: Conclusions

3D culturing lies in its ability to replicate the heterogeneity of drug sensitivity observed in actual tumours. Unlike 2D cultures, Considering the results from the WST-1 cell viability assay, which are highly oxygenated and fully exposed to treatment, senescence staining, western blot analyses of senescence and resulting in rapid drug responses and reactive oxygen species treatment resistance markers, as well as blood analysis, deter- (ROS) accumulation, cells in the hypoxic core of 3D spheroids mining the optimal treatment strategy for this patient remains exhibit greater treatment resistance. These differences in the challenging. The summarised findings in Table 2 highlight con- extracellular matrix (ECM), drug penetration, oxygen and nu- flicting indicators for an appropriate therapeutic approach. trient availability and gene and protein expression profiles make 3D spheroids more accurate representations of the TME. We hypothesised that establishing 3D cultures could offer a more While Dxr demonstrated the most significant reductions in proliferation and cell viability, low-dosage Carbo emerged comprehensive approach to evaluating patient-specific treat- as a potentially effective treatment for eliminating cervical ment responses and predicting the potential for drug resistance. cancer cells while avoiding activation of treatment resistance pathways. However, the increased ABCG2 expression associ-

5.1 ↑ Protocol for Organoid Culturing

ated with Carbo administration raises concerns about its po- tential to induce treatment resistance. In essence, we hoped For organoid culturing, we utilised ClinoStar bioreactors pro- that these results could provide valuable insights to clinicians vided by the South African Medical Research Council (SAMRC). in making well-informed treatment decisions tailored to the individual patient's needs, rather than relying solely on con- These bioreactors facilitate 3D culture by maintaining cells within a continuously rotating vessel filled with culture me-

---CHUNK_BREAK---

TABLE 1 I The patient's whole blood plasma analysis.

	White blood cell (WBC) count	Red blood cell (RBC) count	Platelet count
Normal range	3.71×103/μL-10.67× 103/μL	3.87×106/μL-5.68×10%/μL	150.5×103/μL-366.8×103/μL
Patient results	11.09×103/μL	5.21×10%/μL	231.4×103/μL
Indication as ‘high' or “low' or 'normal'	High	Normal	Normal

---CHUNK_BREAK---

TABLE 2 I Summary of the best treatment options for each experimental variable for the patient.

	Cell viability (WST-1)	Proliferation marker-(MCM2)	Senescence marker-p16	Senescence marker-pRb/total Rb	Treatment resistance marker-MDR1	Treatment resistance marker-ABCG2
Best option	Dxr	Dxr	Dxr	Gem	Pxt	Pxt
Second best option	Carbo + Gem	Carbo	Gem	Dxr	Carbo	Gem

---CHUNK_BREAK---

ventional treatment protocols. Despite the valuable insights gained, experimental limitations and technical challenges
dium. This dynamic environment promotes spheroid formation
necessitated exploring more advanced methodologies, ulti-
while maintaining a stable 3D structure. The ClinoStar system
mately motivating the investigation of 3D organoid cultures
simulates a microgravity-like environment by applying constant rotation and shear forces, creating a suspension state that en-
as a means to overcome these restrictions and enhance thera-
courages uniform cell aggregation and growth. The bioreactor
peutic evaluations.
placement in the bioreactors, the samples were incubated in the
features a central rotating drum and a sealed chamber that pre-
ClinoStar system until they reached an optimal spheroid diameter
cisely controls critical parameters such as oxygen levels, pH and nutrient supply. This setup fosters a stable microenvironment
of approximately 0.2 mm. At this stage, the organoids were ready
for spheroid development, making it particularly effective for
for treatment and further experimental analysis.
regulating organoid size, shape and physiological conditions.
The resulting spheroid cultures are more consistent and repro- ducible, offering a superior representation of tumour conditions
6 | Case Report for Patient X
compared to traditional 2D ex vivo models.
The patient used for the 3D organoid culture, referred to as Patient
In preparation for culturing, biopsy samples were first rinsed with
X, was a 47-year-old HIV-negative South African female diagnosed
HBSS and then cut into smaller fragments, following a proto-
with stage 2B cervical SCC involving the perimetrium at Tygerberg
col similar to the ex vivo cell culture method. Unlike the ex vivo
Hospital, Cape Town. After staging confirmation, she provided in-
model, trypsin was not used to dissociate cells into single-cell
formed consent for a cervical tumour biopsy. Due to limited tissue
suspensions. Instead, intact biopsy fragments were directly dis-
availability, only two treatment groups were used: a control and
tributed across different treatment groups. Ideally, each bioreactor
a carboplatin group, with a 12pM concentration consistent with
would house 4-6 biopsy pieces, but due to the limited size of the
ex vivo experiments. Tumour size analysis and IHC staining for
cervical tumour samples, we used 3-5 pieces per bioreactor. After

---CHUNK_BREAK---

MODE 2: GENERAL FIGURE CONTENT

The image displays a series of microscopic images viewed under different staining conditions, likely to analyze biological structures. The figure shows six panels labeled A through F, each depicting cells or tissues with varying stains and magnifications. The top left panel is titled "CONTROL" and appears to show normal, unstained tissue without any distinct features or structures that can be discerned. In the second row from the top, the rightmost panel is labeled "CARBOPLATIN" and shows tissue with a prominent purple coloration, indicative of a staining process that highlights a specific cellular component. The third panel from the top right, labeled "A", presents a different staining result, with various shades and intensities across the cells and tissue, suggesting the presence of different molecules or proteins.

The bottom left corner features a magnification control labeled "60M," indicating that the image is taken at 60 times magnification. The remaining panels exhibit similar cellular structures but with varying degrees of contrast and color intensity, which could signify variations

in the staining process or the chemical properties of the tissues being examined.

There are no visible texts within the images themselves, such as titles, labels, or annotations. All visible text is part of the figure's external labels and captions. The style of the figure suggests a scientific or medical context, potentially for research or diagnostic purposes.taken using the Nikon ECLIPSE Ti inverted microscope and NIS elements imaging software at 40X and 100x, respectively.
FIGURE 9 I (A-F) IHC staining of treatment resistance marker ABCG2 was done on control and carbo-treated organoid samples. Images were
Carboplatin
Control
D
100µM
100µM
B
40uM
40uM

---CHUNK_BREAK---

the treatment resistance marker ABCG2 were performed.
the need for integrative, multidisciplinary approaches in person-
6.1 I Protocol for Sectioning and
alised medicine.
Immunohistochemistry Staining for Patient X Organoids
7|Conclusions
Patient X's cervical tumour biopsy was cultured in ClinoStar bioreactors for 4weeks until the organoids reached the exper-
While our initial aim was to predict treatment outcomes for indi-
imental size. This lengthy incubation period presented chal-
vidual patients based on ex vivo cell cultures, the variability and
lenges due to time and cost constraints. Moreover, only two
complexity encountered across methods highlighted a broader,
viable organoids per bioreactor remained, limiting experimental
critical insight: no single experimental model can fully encom-
options. As a result, sectioning and IHC staining were priori-
pass the nuances of treatment response in cervical cancer. Even
tised to maximise analysis.
though we could not necessarily aid medical practitioners in the best treatment for the patients to reduce the likelihood of drug
Organoids were embedded in paraffin wax and sectioned with a
resistance, these results could be used in combination with other
microtome. Following deparaffinisation and rehydration, anti-
experimental results in the future—-once they become optimised
gen retrieval was conducted using the PASCAL system. ABCG2
and efficient enough—to aid in decision making. These results
primary antibody (1:300 dilution) was incubated overnight at
highlight the importance of expanding experimental optimisa-
4°C. After rinsing, HRP-conjugated secondary antibody was ap-
tion and incorporating multiple methodologies when applying
plied for 30 min, followed by DAB chromogen for visualisation.
personalised medicine, particularly in resource-limited regions
The sections were counterstained with haematoxylin, dehy-
like South Africa.
drated, mounted with coverslips and examined microscopically to assess protein expression.
While the ex vivo 2D and 3D organoid models demonstrate promising predictive potential, these findings have yet to
6.2 I Analysis of Treatment Resistance Protein
be correlated with long-term clinical outcomes, such as progression-free survival or overall survival. Consequently, fu-

Expression Using Organoid Cultures

ture studies are crucial to fully assess the applicability of per- sonalised medicine in LMICs. This need is underscored by the

---CHUNK_BREAK---

Analysis of the sample revealed no statistically significant in-
limited availability of molecular diagnostics, high-throughput
crease in the expression of ABCG2 ($p<0.05$) compared to the
sequencing platforms, and biobanking infrastructure in these
patient control, as shown in Figure 9.
settings. These constraints highlight the importance of devel-
Although no positive ABCG2 staining was observed, carbopla-
oping simplified, scalable and cost-effective screening tools that can be feasibly implemented within public healthcare systems.
tin treatment reduced organoid size by approximately 80% com-
However, even though initial investment costs for incorporat-
pared to the control (Figure 10).
ing personalised medicine into the public healthcare system
Using the 3D organoid model aimed to enhance treatment anal-
may be high, there is growing recognition that such approaches offer considerable long-term benefits to all key stakeholders by
ysis based on ex vivo results. However, culturing challenges,
introducing technologies that improve diagnosis, prognosis and
bioreactor limitations and unclear antibody staining highlighted
treatment; ultimately reducing the number of patients requir- ing prolonged care and lowering the incidence of adverse drug responses [41].

Additionally, recent advances in organoid technology have demonstrated their potential for modelling tumour architecture and drug response and investigating immune-tumour interac- tions [42]. Although the 3D organoid models used in this study do not include immune system components, multiple studies have shown that such integration is feasible and valuable. For instance, co-culturing patient-derived organoids with autolo- gous peripheral blood mononuclear cells (PBMCs) has enabled the expansion of T cells capable of targeting matched tumour organoids, effectively modelling immune-mediated cytotoxicity [43]. These models retain key genetic and histological features of the original tumour, allowing for the assessment of personalised responses to immunotherapies, including immune checkpoint inhibitors. Incorporating immune components such as T cells or tumour-infiltrating lymphocytes (TILs) into cervical cancer patient-derived models could enhance their predictive power and relevance for guiding treatment decisions, especially as immunotherapies continue to gain traction in gynaecological oncology. Future work should explore such integrated models to broaden the utility of organoid-based personalised medicine,

---CHUNK_BREAK---

1. Visual Type: Bar chart.
2. Title: Patient X % shrinkage.
3. Axes / Legends / Labels:
   - Vertical axis labeled "Percentage of shrinkage".
4. Data Points: There are three bars visible, each representing a different treatment or group. The bar heights correspond to the amount of shrinkage measured in percentage.
5. Captions / Annotations: There is no visible text providing captions or annotations for specific data points or features.(FIJI) analysis software.

pared to the control ($p<0.05$). Size analysis was done using ImageJ
face area of the organoids was seen in the carbo treatment group com-
with carbo compared to the control. A significant reduction in the sur-
FIGURE 10 | Percentage shrinkage of the organoids after treatment
PatientX
% shrinkage
✳
150

con
100-
to
ed
50
com
5
Treatment groups

---CHUNK_BREAK---

2045 7634,
4. A. Hernandez-Segura, J. Nehme, and M. Demaria, “Hallmarks of
particularly in resource-limited settings where streamlined pre-
2025,
Cellular Senescence," Trends in Cell Biology 28 (2018): 436-453, https:/
dictive tools could significantly impact treatment stratification.
doi.org/10.1016/j.tcb.2018.02.001.
13,
This study underscores the value of such an integrative ap-
5. D. McHugh and J. Gil, “Senescence and Aging: Causes, Conse- quences, and Therapeutic Avenues," Journal of Cell Biology 217
(2018):
proach to comprehensively understand treatment resistance
65-77, https://doi.org/10.1083/jcb.201708092.
mechanisms, advocating for carefully designed strategies in
6. X. Chao, J. Fan, X. Song, et al., “Diagnostic Strategies for Recurrent
personalised medicine research.
Cervical Cancer: A Cohort Study,” Frontiers in Oncology 10 (2020): 1253.
7. M. Kosheeka, “Mastering the Challenges of Primary Cell Culture," 2024 Kos (accessed November 1, 2024),
https://www.kosheeka.com/
Author Contributions
mastering-the-challenges-of-primary-cell-culture-unlocking-true-in-
Madre Meyer: investigation, writing - original draft, methodology,
vivo-insights/.
writing - review and editing, formal analysis, visualization. Carla
8. N. Kubo, S.-E. Noda, A. Takahashi, et al., “Radiosensitizing Effect of
Eksteen: conceptualization, investigation, validation, methodol-
Carboplatin and Paclitaxel to Carbon-Ion Beam Irradiation in the Non-
ogy, writing - review and editing, project administration, supervi-
Small-Cell Lung Cancer Cell Line H460," Journal of Radiation Research
sion. Cayleigh de Sousa: investigation, methodology, data curation.
56 (2015): 85, https://doi.org/10.1093/jrr/rru085.
Nireshni Chellan: investigation, methodology, resources, data cu- ration. Ruzayda Van Aarde: investigation, methodology, data cura-

---CHUNK_BREAK---

9. K. Oyama, Y. Iwagami, S. Kobayashi, et al.,"Removal of Gemcitabine-
tion, resources. Meenal Bhaga: investigation, methodology. Johann
Induced Senescent Cancer Cells by Targeting Glutaminasel Improves
Riedemann: conceptualization, validation. Matthys H. Botha: in-
the Therapeutic Effect in Pancreatic Ductal Adenocarcinoma,"" Interna-
vestigation, resources, methodology. Frederick H. van der Merwe:
tional Journal of Cancer 154 (2024): 912-925, https://doi.org/10.1002/

investigation, methodology, resources. Anna-Mart Engelbrecht: con-
ijc.34725.
ceptualization, funding acquisition, validation, writing - review and
10. B. Wang, J. Kohli, and M. Demaria, “Senescent Cells in Cancer Ther-
editing, project administration, supervision, resources.
apy: Friends or Foes?," Trends in Cancer 6 (2020): 838-857, https://doi.
org/10.1016/j.trecan.2020.05.004.

Acknowledgments

11. K. Itahana, Y. Itahana, and G. P. Dimri, “Colorimetric Detection of
Declaration of Generative AI and AI-assisted technologies in the writ-
Senescence-Associated β Galactosidase,” Methods in Molecular Biology
ing process: During the preparation of this work, the authors did not use
965 (2013): 143-156, https://doi.0rg/10.1007/978-1-62703-239-1_8.
any AI-assisted technology.
12. M. Arbyn, E. Weiderpass, L. Bruni, et al., "Estimates of Incidence and Mortality of Cervical Cancer in 2018: A Worldwide Analysis,” Lan-

Ethics Statement

cet Global Health 8 (2020): e191-e203, https://doi.org/10.1016/S2214 -109X(19)30482-6.
Stellenbosch University (HREC—N22/04/037) granted ethical approval for this study.
13. H. Onohuean, E. O. Aigbogun, and B. E. Igere, “Meta-Synthesis and Science Mapping Analysis of HIV/HPV Co-Infection: A Global Perspec- tive With Emphasis on Africa," Globalization and Health 18 (2022): 36,

---CHUNK_BREAK---

Consent

https://doi.org/10.1186/s12992-022-00812-w.
Written informed consent was obtained from the patient to publish this
14. C. A. Burmeister, S. F. Khan, G. Schafer, et al., “Cervical Cancer
case report and accompanying images. A copy of the written consent
Therapies: Current Challenges and Future Perspectives,” Tumour Virus
is available for review by the Editor-in-Chief of this journal on request.
Research 13 (2022): 200238, https://doi.org/10.1016/j.tvr.2022.200238.
15. N. Bano, M. 1. Ansari, K. M. Kainat, V. K. Singh, and P. K. Sharma,

Conflicts of Interest

"Chloroquine Synergizes Doxorubicin Efficacy in Cervical Cancer Cells
The authors declare no conflicts of interest.
Through Flux Impairment and Down Regulation of Proteins Involved in the Fusion of Autophagosomes to Lysosomes,” Biochemical and Bio- physical Research Communications 656 (2023): 131-138, https://doi.org/

Data Availability Statement

10.1016/j.bbrc.2023.03.048.
Data sharing not applicable to this article as no datasets were generated
16. K. Johnson-Arbor and R. Dubey, Doxorubicin (StatPearls Publish-
or analysed during the current study.
ing, 2024).
17. G. Jin, J. Zhao, H. Qi, et al., “Gemcitabine and Carboplatin Demon- strate Synergistic Cytotoxicity in Cervical Cancer Cells by Inhibiting

References

DNA Synthesis and Increasing Cell Apoptosis,” Oncotargets and Ther-
1. D. Singh, J. Vignat, V. Lorenzoni, et al., “Global Estimates of Inci-
apy 6 (2013): 1707-1717, https://doi.org/10.2147/OTT.S54217.
dence and Mortality of Cervical Cancer in 2020: A Baseline Analysis of
18.A. Duenas-Gonzalez, C. Lopez-Graniel, A. Gonzalez, et al., “A

---CHUNK_BREAK---

the WHO Global Cervical Cancer Elimination Initiative," Lancet Global
Phase II Study of Gemcitabine and Cisplatin Combination as Induction
Health 11 (2022): e197-e206, https://doi.org/10.1016/S2214-109X(22)
Chemotherapy for Untreated Locally Advanced Cervical Carcinoma,"
00501-0.
Annals of Oncology 12 (2001): 541-547, https://doi.org/10.1023/A:10111
2. R. Hull, M. Mbele, T. Makhafola, et al., "Cervical Cancer in Low and
17617514.
Middle-Income Countries (Review)," Oncology Letters 20 (2020): 2058-
19. L. Fei and H. Xu, "Role of MCM2-7 Protein Phosphorylation in
2074, https://doi.0rg/10.3892/ol.2020.11754.
Human Cancer Cells," Cell & Bioscience 8 (2018): 43, https://doi.org/10.
3. L. Yang, M.-C. Boily, M. M. Ronn, et al., "Regional and Country-Level
1186/s13578-018-0242-2.
Trends in Cervical Cancer Screening Coverage in Sub-Saharan Africa:
20. H. Safwan-Zaiter, N. Wagner, and K.-D. Wagner, "P16INK4A—
A Systematic Analysis of Population-Based Surveys (2000-2020)," PLoS Medicine 20 (2023): e1004143,
https://doi.org/10.1371/journal.pmed.
More Than a Senescence Marker," Life (Basel) 12 (2022): 1332, https:// doi.org/10.3390/life12091332.
1004143.
2045 7634,
21. Y. Li, S. Xiao, L. Dan, and M. Xue, "P16INK4A Is Required for Cis-
Variations," Scientific Reports 13 (2023): 18380, https:/doi.org/10.1038/
2025,
platin Resistance in Cervical Carcinoma SiHa Cells," Oncology Letters 9

---CHUNK_BREAK---

s41598-023-45144-w.
(2015): 1104-1108, https://doi.org/10.3892/ol.2014.2814.
13,
39. J. C. Fontoura, C. Viezzer, F. G. dos Santos, et al., "Comparison of 2D and 3D Cell Culture Models for Cell Growth, Gene
Expression and Drug
22. J. Guillon, C. Petit, B. Toutain, C. Guette, E. Lelievre, and O. Co- queret, "Chemotherapy-Induced Senescence, an Adaptive
Mechanism
Resistance," Materials Science and Engineering: C 107 (2020): 110264,
Driving Resistance and Tumor Heterogeneity" Cell Cycle 18 (2019):
https:/doi.org/10.1016/j.msec.2019.110264.
2385-2397, https://doi.0rg/10.1080/15384101.2019.1652047.
40. M. Kapalczynska, T. Kolenda, W. Przybyla, et al., "2D and 3D Cell Cultures—-A Comparison of Different Types of Cancer Cell
Cultures,"
23. S. Purohit, W. Zhi, D. G. Ferris, et al., "Senescence-Associated Se- cretory Phenotype Determines Survival and Therapeutic
Response in
Archives of Medical Science 14 (2018): 910-919, https://doi.org/10.5114/
Cervical Cancer," Cancers (Basel) 12 (2020): 2899, https://doi.org/10.
aoms.2016.63743.
3390/cancers12102899.
41. B. Godman, A. E. Finlayson, P. K. Cheema, et al., "Personalizing
24. M. Bossennec, A. Di Roio, C. Caux, and C. Ménetrier-Caux, "MDR1
Health Care: Feasibility and Future Implications," BMC Medicine 11
in Immunity: Friend or Foe?" Oncoimmunology 7 (2018): e1499388,
(2013): 179, https://doi.0rg/10.1186/1741-7015-11-179.

---CHUNK_BREAK---

https://doi.0rg/10.1080/2162402X.2018.1499388.
42. S. Gunti, A. T. K. Hoke, K. P. Vu, and N. R. London, “Organoid and
25. W. Chen, “Correlation Between the Expression of ABCG2 in Cervi-
Spheroid Tumor Models: Techniques and Applications,” Cancers 13 (2021): 874, https://doi.org/10.3390/cancers13040874.
cal Cancer Tissues and the Clinicopathological Parameters and Prog- nosis of Patients With Cervical Cancer,”Acta Medica Mediterranea 67
43. M. Morales-Martinez and M. I1. Vega, ""p38 Molecular Targeting for
(2020): 1483-1487, https://doi.0rg/10.19193/0393-6384_2020_3_231.
Next-Generation Multiple Myeloma Therapy," Cancers 16 (2024): 256,
26. M. Ding, H. Zhang, L. Liu, and R. Liang, “Effect of NOS1 Regulating
https://doi.org/10.3390/cancers16020256.
ABCG2 Expression on Proliferation and Apoptosis of Cervical Cancer Cells," Oncology Letters 17 (2019): 1531-1536, https://doi.org/10.3892/0l.
2018.9786.
27. F. Yang, B. Gao, R. Li, et al., “Expression Levels of Resistant Genes Affect Cervical Cancer Prognosis,” Molecular Medicine Reports 15 (2017): 2802-2806, https://doi.org/10.3892/mmr.2017.6328.
28. J. Ke, C. Gu, H. Zhang, et al., “Nucleolin Promotes Cisplatin Resis- tance in Cervical Cancer by the YB1-MDR1 Pathway," Journal of Oncol- ogy 2021 (2021): 9992218, https://doi.org/10.1155/2021/9992218.
29. E. Tharavichitkul, V. Lorvidhaya, P. Kamnerdsupaphon, et al., "Combined Chemoradiation of Cisplatin Versus Carboplatin in Cervical Carcinoma: A Single Institution Experience From Thailand,” BMC Cancer 16 (2016): 501, https://doi.org/10.1186/s12885-016-2558-9.

---CHUNK_BREAK---

30. A. Vitkauskaite, D. Urboniene, J. Celiesiute, et al., “Expression of Inflammation Depending on the Stage of Cervical Cancer,” Medicina 60 (2024): 349, https://doi.0rg/10.3390/medicina60030349.
31. A. Vitkauskaite, D. Urboniene, J. Celiesiute, et al., “Circulating Inflammatory Markers in Cervical Cancer Patients and Healthy Controls," Journal of Immunotoxicology 17 (2020): 105-109, https://doi.org/ 10.1080/1547691X.2020.1755397.
32. M. K. Kordi Tamandani, R. C. Sobti, M. Shekari, M. Mukesh, and V.
Suri, “Expression and Polimorphism of IFN-Gamma Gene in Patients With Cervical Cancer,” Experimental Oncology 30 (2008): 224-229.
33. Y. Yang and Y. Cao, “The Impact of VEGF on Cancer Metastasis and Systemic Disease,” Seminars in Cancer Biology 86 (2022): 251-261, https://doi.org/10.1016/j.semcancer.2022.03.011.
34. J. Zhang, J. Liu, C. Zhu, et al., “Prognostic Role of Vascular Endothe- lial Growth Factor in Cervical Cancer: A Meta-Analysis,” Oncotarget 8 (2017): 24797-24803, https://doi.org/10.18632/oncotarget.15044.
35. C. H. Choi, H. Kang, W. Y. Kim, et al., “Prognostic Value of Baseline Lymphocyte Count in Cervical Carcinoma Treated With Concurrent Chemoradiation,” International Journal of Radiation Oncology, Biology, Physics 71 (2008): 199-204, https://doi.0rg/10.1016/j.ijrobp.2007.09.024.
36. F. Shi, A. K. Yoder, C. Mach, et al., “Impact of Hematologic Toxic- ities During Concurrent Chemoradiation for Cervical Cancer,” Obstet- rics & Gynecology Science 65 (2022): 176-187, https://doi.org/10.5468/ ogs.21308.

---CHUNK_BREAK---

37. S. A. Battistini Garcia and N. Guzman, Acquired Immune Deficiency Syndrome CD4+ Count (StatPearls Publishing, 2024).
38. Z. N. Abbas, A. Z. Al-Saffar, S. M. Jasim, and G. M. Sulaiman, "Comparative Analysis Between 2D and 3D Colorectal Cancer Culture Models for Insights Into Cellular Morphological and Transcriptomic